Histopathology

Histopathology 2021 DOI: 10.1111/his.14378

Bcl-2-negative *IGH-BCL2* translocation-negative follicular lymphoma of the thyroid differs genetically and epigenetically from Bcl-2-positive *IGH-BCL2* translocation-positive follicular lymphoma

Yuichiro Hamamoto,[1,2] Yoji Kukita,[3] Masanori Kitamura,[1] Masako Kurashige,[2] Hiroaki Masaie,[4] Shigeo Fuji,[4] Jun Ishikawa,[4] Keiichiro Honma,[1] Tomoko Wakasa,[5] Hitoshi Hanamoto,[6] Mitsuyoshi Hirokawa,[7] Ayana Suzuki,[7] Eiichi Morii[2] & Shin-ichi Nakatsuka[8]

[1]*Department of Diagnostic Pathology and Cytology, Osaka International Cancer Institute,* [2]*Department of Pathology, Osaka University Graduate School of Medicine,* [3]*Laboratory of Genomic Pathology, Osaka International Cancer Institute,* [4]*Department of Hematology, Osaka International Cancer Institute, Osaka,* [5]*Diagnostic Pathology and Laboratory Medicine, Kindai University Nara Hospital,* [6]*Department of Hematology, Kindai University Nara Hospital, Nara,* [7]*Department of Diagnostic Pathology and Cytology, Kuma Hospital, Hyogo, and* [8]*Department of Pathology, Sakai City Medical Center, Osaka, Japan*

Date of submission 21 August 2020
Accepted for publication 4 April 2021
Published online *Article Accepted* 7 April 2021

Hamamoto Y, Kukita Y, Kitamura M, Kurashige M, Masaie H, Fuji S, Ishikawa J, Honma K, Wakasa T, Hanamoto H, Hirokawa M, Suzuki A, Morii E & Nakatsuka S-I (2021) *Histopathology*. https://doi.org/10.1111/his.14378

Bcl-2-negative *IGH-BCL2* translocation-negative follicular lymphoma of the thyroid differs genetically and epigenetically from Bcl-2-positive *IGH-BCL2* translocation-positive follicular lymphoma

Aims: Follicular lymphoma (FL), comprising a minor subset of primary thyroid lymphomas, is divided into two groups based on Bcl-2 expression and *IGH-BCL2* translocation. The clinicopathological features exhibited by Bcl-2-negative *IGH-BCL2* translocation-negative FL of the thyroid (Bcl-2^{-}/*IGH-BCL2*$^{-}$ tFL) are different from those of conventional FL; however, its lymphomagenesis remains unclear. Here, we collected samples from seven patients with Bcl-2^{-}/*IGH-BCL2*$^{-}$ tFL to investigate their epigenetic and genetic aberrations.

Methods and results: The immunohistochemical profiles of epigenetic modifiers and the methylation status of histones were examined, including EZH2, MLL2/KMT2D, CBP/CREBBP, EP300, H3K27me3 and H3K4me3, in Bcl-2^{-}/*IGH-BCL2*$^{-}$ tFL and Bcl-2-positive *IGH-BCL2* translocation-positive FL of the thyroid (Bcl-2^{+}/*IGH-BCL2*$^{+}$ tFL). Most Bcl-2^{-}/*IGH-BCL2*$^{-}$ tFLs retained the positivity of epigenetic modifiers and lower expression of H3K27me3, although Bcl-2^{+}/*IGH-BCL2*$^{+}$ tFLs exhibited aberrant immunohistochemical patterns of EZH2 and CBP/CREBBP and overexpression of H3K27me3. Samples from seven cases were further analysed using targeted sequencing, focusing on the exons of 409 key tumour suppressor genes and oncogenes. Bcl-2^{-}/*IGH-BCL2*$^{-}$ tFLs do not have pathogenic mutations of epigenetic modifiers, such as *EZH2*, *MLL2/KMT2D*, *MLL3/KMT2C*, *EP300* and *ARID1A*, which have been reported in FLs in the literature, whereas Bcl-2^{+}/*IGH-BCL2*$^{+}$ tFLs are probably pathogenic/pathogenic missense mutations or frameshift mutations of these genes. Additionally, novel mutations in *TET2* and *EP400* were detected in Bcl-2^{-}/*IGH-BCL2*$^{-}$ tFLs.

Conclusions: Different genetic and epigenetic abnormalities might be involved in the oncogenesis of Bcl-2^{-}/*IGH-BCL2*$^{-}$ tFLs from Bcl-2^{+}/*IGH-BCL2*$^{+}$ tFLs and other FLs.

Address for correspondence: Shin-ichi Nakatsuka, Department of Pathology, Sakai City Medical Center, 1-1-1 Ebaraji-cho, Nishi-ku, Sakai, Osaka 593-8304, Japan. e-mail: s-nakatsuka@sakai-hospital.jp

© 2021 John Wiley & Sons Ltd.

Keywords: Bcl-2, epigenetics, follicular lymphoma, thyroid

Introduction

Primary thyroid lymphoma (PTL) is a relatively rare neoplasm that accounts for 1–5% of thyroid malignancies.[1] B cell PTLs include diffuse large B cell lymphoma, extranodal marginal zone B cell lymphoma of mucosa-associated lymphoid tissue type (MALT lymphoma), follicular lymphoma (FL), small lymphocytic lymphoma and Burkitt lymphoma. Diffuse large B cell and MALT lymphomas are the most frequently observed B cell PTLs, followed by FL.[2] Most PTLs are closely associated with preceding autoimmune lymphocytic thyroiditis (Hashimoto's disease).[3]

Bacon et al.[3] demonstrated that thyroid follicular lymphoma can be clearly divided into two groups according to their clinical, morphological, immunophenotypical and genetic features. The features of the first group are the presence of $t_{(14;18)}$/*IGH-BCL2* translocation and/or Bcl-2 expression, high CD10 positivity and World Health Organisation (WHO) grades 1–2, whereas those of the second group are the absence of $t_{(14;18)}$/*IGH-BCL2* translocation and Bcl-2 expression, high CD10 negativity and WHO grade 3. The molecular pathogenesis of this disease has not been fully investigated.

Recently, frequent mutations of epigenetic modifiers, including *EZH2*, *MLL2*/*KMT2D*, *CBP*/*CREBBP*, *EP300* and *MEF2B*, have been described in FL.[4] Gain-of-function mutations in *EZH2* promote methylation at lysine 27 of histone H3, thus suppressing the transcription of anti-oncogenic genes (ex. *CDKN1A*, *CDKN2A* and *PRDM1*) and promoting the expression of oncogenic genes (ex. *IRF4*). Loss-of-function mutations in *MLL2*/*KMT2D* result in demethylation of the lysine located at position 4 of H3 and subsequent gene suppression (ex. *TNFAIP3*, *SOCS3* and *TNFRSF14*). Loss-of-function mutations in both *CBP*/*CREBBP* and *EP300* (*CBP*/*EP300* complex) leads to deacetylation of the lysine of H3, and subsequent suppression of major histocompatibility complex (MHC) class II and acetylation of non-histone proteins (p53 and Bcl-6).

We compared the clinicopathological characteristics of Bcl-2-negative *IGH-BCL2* translocation-negative FL of the thyroid (Bcl-2^-/*IGH-BCL2*$^-$ tFL) and Bcl-2-positive *IGH-BCL2* translocation-positive FL of the thyroid (Bcl-2^+/*IGH-BCL2*$^+$ tFL) and examined the differences in the expression of epigenetic modifiers and methylation status. We also analysed genetic aberrations to elucidate the differences in oncogenesis between these two diseases.

Materials and methods

PATIENTS

We selected seven patients with Bcl-2^-/*IGH-BCL2*$^-$ tFL and four patients with Bcl-2^+/*IGH-BCL2*$^+$ tFL from the pathological database (from 2013 to 2019) of the Osaka International Cancer Institute (OICI), Osaka University Hospital, Kindai University Nara Hospital and Kuma Hospital. Additionally, as control samples, five cases with nodal Bcl-2^+ FL and three cases with reactive lymphoid hyperplasia from OICI were included in our study. This study was approved by the Ethical Review Boards of OICI (no. 19031), Osaka University Hospital (no. 20050 and no. 20305), Kindai University Nara Hospital (no. 603) and Kuma Hospital (no. 20201008-3). All experiments were performed in accordance with the guidelines and regulations of all the committees.

IMMUNOHISTOCHEMISTRY

All tissue samples were fixed in 10% formalin, embedded in paraffin, cut into 4-μm-thick serial sections and used for haematoxylin and eosin staining and immunohistochemical staining. The latter was performed using the Roche BenchMark ULTRA IHC/ISH staining module (Ventana Medical Systems, Tucson, AZ, USA), according to the manufacturer's instructions. The primary antibodies used in this study and their dilution ratios are listed in Table 1. Immunohistochemical staining was scored by two independent pathologists (Y.H. and S.N.). Weak positivity was defined as weaker staining than that of the positive control cells or internal control cells (Table 1). Focal positivity was defined as a positivity rate of $< 50\%$. Cases which fulfilled the following criteria were classified as 'negative': (1) less than 10% of the positivity rate and (2) weak-to-null intensity. Regarding Bcl-2, we estimated the net positivity rate in neoplastic B cells in germinal centres.

© 2021 John Wiley & Sons Ltd, *Histopathology*

Table 1. Primary antibodies used in this study

Antibody	Clone	Dilution	Manufacturer	Control cells
CD20	L26	RTU	Roche	B cells
CD3	2GV6	RTU	Roche	T cells
CD5	SP19	RTU	Roche	T cells
CD10	56C6	RTU	Leica (Novocastra)	Germinal centre B cells
Bcl-2	SP66	RTU	Roche	Mantle zone B cells
Bcl-6	GI191E/A8	RTU	Roche	Germinal centre B cells
LMO2	SP51	RTU	Roche	Germinal centre B cells
HGAL	MRQ-49	RTU	Roche	Germinal centre B cells
MUM1	MRQ-43	RTU	Roche	DLBCL (ABC)
IRTA1 (FCRL4)	EPR21961	1:100	abcam	MALT lymphoma
CD23	SP23	RTU	Roche	Follicular dendritic cells
C-myc	Y69	RTU	Roche	Burkitt lymphoma
MIB-1	Mib-1	1:500	Agilent (Dako)	Germinal centre B cells
EZH2	D2C9	1:200	Cell Sigalling Technology	Germinal centre B cells
MLL2/KMT2D	Polyclonal	1:200	Sigma-Aldrich	Germinal centre B cells
CBP/CREBBP	C-1	1:100	Santa Cruz Biotechnology	Germinal centre B cells
EP300	D8Z4E	1:1000	Cell Signaling Technology	Germinal centre B cells
H3K27me3	C36B11	1:200	Cell Signaling Technology	Vascular endothelial cells
H3K4me3	Polyclonal	1:100	Cell Signaling Technology	Germinal centre B cells

RTU, ready to use; DLBCL (ABC), diffuse large B cell lymphoma (activated B cell); MALT, mucosa-associated lymphoid tissue.

ANALYSES FOR *IGH-BCL2* REARRANGEMENT AND *IGH* CLONAL REARRANGEMENT USING POLYMERASE CHAIN REACTION (PCR) AND FLUORESCENT *IN-SITU* HYBRIDISATION (FISH)

To analyse the *IGH-BCL2* rearrangement status, we performed PCR-based studies and FISH analyses using tumour tissues. Briefly, for PCR, sections cut from paraffin-embedded specimens were processed by deparaffinisation, and DNA was extracted. We assessed *IGH-BCL2* rearrangement according to modified BIOMED-2 protocols.[5,6] For FISH, analyses were performed on paraffin sections using the BOND FISH kit (Leica Biosystems Newcastle Ltd, Newcastle upon Tyne, UK), Kreatech XL probe (BCL2 (18q21) Break, BOND enzyme pretreatment kit, BOND hybridisation solution and BOND-III, according to the manufacturer's instructions. We also performed *IGH* clonal rearrangement analyses on the extracted DNA according to the modified BIOMED-2 protocols.

TARGETED SEQUENCING

Informed consent was obtained from four of the seven patients diagnosed with Bcl-2^{-}/*IGH-BCL2*$^{-}$ tFL and from three of four patients diagnosed with Bcl-2^{+}/*IGH-BCL2*$^{+}$ tFL for targeted sequencing studies. DNA extraction from paraffin-embedded specimens and targeted sequencing were performed by Macrogen Japan Corporation (Kyoto, Japan). The Ion AmpliSeq Comprehensive Cancer Panel (Thermo Fisher Scientific Inc., Waltham, MA, USA) was used to analyse the exons of 409 key tumour suppressor genes and oncogenes (Supporting information, Table S1).

VARIANT DATA ANALYSIS

We used the following filtering parameters for variant selection: (1) total coverage ≥ 20, (2) variant allele coverage ≥ 10, (3) variant allele fraction $\geq 5\%$, (4) variants with both forward and reverse reads and (5)

© 2021 John Wiley & Sons Ltd, *Histopathology*

non-synonymous or splice-site variants. To remove probable germline variants, we used allele frequency information available from public polymorphic variant databases and excluded any variants that possessed an observed allele frequency ≥ 0.5% in any of the ethnic populations in gnomAD exome (version 2.0.1), gnomAD genome (version 2.0.1),[7] 1000 genomes (August 2015 collection),[8] National Heart, Lung, and Blood Institute (NHLBI) Exome Sequencing Project with 6500 exomes,[9] 4.7KJPN Allele Frequency Panel (version 20190826) from the Tohoku Medical Megabank Organisation (ToMMo)[10] and Human Genetic Variation Database (HGVD) (version 2.30) from Kyoto University[11] using ANNOtate VARiation (ANNOVAR).[12] Data sets for ToMMo[13] and HGVD[14] were used. Other data sets were downloaded from the ANNOVAR site.[15] Additionally, variants exhibiting greater than 95% variant allele fraction were excluded from the analysis, as seven patients had no family history of cancer.

Results

CLINICAL FINDINGS

The clinical findings of the seven cases with Bcl-2$^-$/*IGH-BCL2*$^-$ tFL and four cases with Bcl-2$^+$/*IGH-BCL2*$^+$ tFL are summarised in Table 2. Both groups showed a female predilection. The mean age of the patients with Bcl-2$^-$/*IGH-BCL2*$^-$ tFL and Bcl-2$^+$/*IGH-BCL2*$^+$ tFL was 71 and 63 years, respectively. Five of seven patients with Bcl-2$^-$/*IGH-BCL2*$^-$ tFL had antecedent autoimmune thyroiditis, whereas only one of four patients with Bcl-2$^+$/*IGH-BCL2*$^+$ tFL had it. All thyroid FLs were localised regardless of the Bcl-2/*IGH-BCL2* status. None of the patients died because of tumour progression. In case 3, a recurrent tumour was detected and resected repeatedly.

HISTOLOGICAL FINDINGS

All Bcl-2$^-$/*IGH-BCL2*$^-$ tFLs and Bcl-2$^+$/*IGH-BCL2*$^+$ tFLs exhibited enlarged neoplastic follicles with attenuated mantle zones. Moderate- to large-sized lymphoid cells that consisted of centrocyte-like or centroblast-like cells proliferated in the absence of tingible body macrophages in expanding germinal centres. In Bcl-2$^-$/*IGH-BCL2*$^-$ tFLs mitotic figures were frequent and all seven cases were classified as WHO grades 2 or 3A, whereas in Bcl-2$^+$/*IGH-BCL2*$^+$ tFLs, mitotic figures were rare and the WHO grade varied among the cases (Table 3 and Figure 1).

IMMUNOHISTOCHEMISTRY

The immunohistochemical findings for tFLs are shown in Tables 3 and 4. In patients with Bcl-2$^-$/*IGH-BCL2*$^-$ tFL (cases 1–7), neoplastic lymphoid cells were positive for CD20 and Bcl-6 and negative for CD3 and Bcl-2. The expression of CD10 was decreased; however, the expression levels of Bcl-6, LMO2 and HGAL were retained (Figure 2A–F). The MIB-1 labelling index ranged from 60 to 90%. In patients with Bcl-2$^+$/*IGH-BCL2*$^+$ tFLs (cases 8–11), neoplastic lymphoid cells were positive for CD10 and Bcl-2 and the MIB-1 labelling index ranged from 20 to 40%.

The comparison of the immunohistochemical analyses for epigenetic modifiers and the methylation status of histones in Bcl-2$^-$/*IGH-BCL2*$^-$ tFL (cases 1–7, Figure 3A–D) and Bcl-2$^+$/*IGH-BCL2*$^+$ tFL (cases 8–11, Figure 3E–H) are summarised in Table 4.

In Bcl-2$^-$/*IGH-BCL2*$^-$ tFL, positivity for EZH2, MLL2/KMT2D, CBP/CREBBP and EP300 were retained except in one case (case 1) that exhibited a lower positivity of EZH2, whereas in Bcl-2$^+$/*IGH-BCL2*$^+$ tFL, EZH2 positivity was decreased in all cases and CBP/CREBBP was negative in two of four cases (cases 9 and 11). In Bcl-2$^+$/*IGH-BCL2*$^+$ tFL, three of four cases exhibited an increased expression of H3K27me3, whereas in Bcl-2$^-$/*IGH-BCL2*$^-$ tFL, all cases exhibited no or low-level expression (cases 3, 4 and 7). All but one case (case 1) retained H3K4me3 expression in both groups of thyroid FL regardless of Bcl-2 status.

ANALYSES FOR *IGH-BCL2* REARRANGEMENT AND *IGH* CLONAL REARRANGEMENT USING PCR AND FISH

Clonal *IGH* rearrangement was detected in all but one case with Bcl-2$^-$/*IGH-BCL2*$^-$ tFL and Bcl-2$^+$/*IGH-BCL2*$^+$ tFL (Table 5). The *BCL2* rearrangement status examined using the PCR-based study and FISH analysis is shown in Table 5.

TARGETED SEQUENCING

Recurrently mutated genes ranked in the top 15 and *EZH2* and *EP300* are presented in Figure 4. Bcl-2$^-$/*IGH-BCL2*$^-$ tFL cases had no probable pathogenic/-pathogenic mutations of epigenetic modifiers and linker histones, including *EZH2*, *MLL2*/*KMT2D*, *MLL3*/*KMT2C*, *EP300* and *ARID1A*, although pathogenic mutations of these genes have been previously reported in FLs. Probable pathogenic/pathogenic

© 2021 John Wiley & Sons Ltd, *Histopathology*

© 2021 John Wiley & Sons Ltd, *Histopathology*

Table 2. Clinical findings

No.	Age (years)	Sex	Tumour size (mm)	Autoimmune thyroiditis	sIL-2R (U/ml)	LDH (U/l)	BM involvement	Leukaemic picture in PB	Clinical stage	B symptoms	Treatment	Survival
Bcl-2^{-}//*IGH-BCL2*$^{-}$ tFL												
1	79	F	50 × 40	+	482	202	–	–	IE	–	RT	Alive at 2 years 4 months, NED
2	69	F	39 × 33 × 23	+	472	250	–	–	IE	ND	R-CHOP	Alive at 1 year 5 months, NED
3	73	F	12 × 11 × 7	+	220	184	ND	–	ND	ND	Observation	Alive at 5 years 2 months, recurrence
4	77	F	36 × 35 × 18	–	432	197	–	–	IIE	–	RT	Alive at 3 years 0 months, NED
5	47	M	35 × 18 × 14	+	663	270	ND	–	ND	ND	R-CHOP	ND
6	81	F	32 × 22 × 13	–	568	237	ND	–	ND	–	R-CVP	Alive at 3 years 5 months, NED
7	55	F	68 × 53	+	419	157	ND	–	ND	–	Observation	Alive at 1 year 0 months, NED
Bcl-2^{+}//*IGH-BCL2*$^{+}$ tFL												
8	58	F	21 × 18 × 14	+	224	156	ND	-	I	-	Resection and observation	Alive at 3 years 2 months, NED
9	62	F	28 × 18 × 9	-	476	249	ND	-	III at least	-	R-B	Alive at 2 years 5 months, CMR
10	66	F	19 × 8 × 13	-	238	159	ND	-	IE	-	Resection	Alive at 6 years 7 months, NED
11	66	F	24 × 10 × 18	-	441	208	ND	-	IIE	-	Resection and R-CHOP	Alive at 7 years 0 months, NED

Bcl-2^{-}//*IGH-BCL2*$^{-}$ tFL, Bcl-2-negative *IGH-BCL2* translocation-negative follicular lymphoma of the thyroid; Bcl-2^{+}//*IGH-BCL2*$^{+}$ tFL, Bcl-2-positive *IGH-BCL2* translocation-positive follicular lymphoma of the thyroid; sIL-2R, soluble interleukin-2 receptor; BM, bone marrow; ND, no data; PB, peripheral blood; RT, radiation therapy; R-CHOP, chemotherapy with rituximab, cyclophosphamide, doxorubicin hydrochloride (hydroxydaunorubicin), vincristine (oncovin), and prednisone; R-CVP, chemotherapy with rituximab, cyclophosphamide, vincristine (oncovin), and prednisone; R-B, chemotherapy with rituximab and bendamustine; NED, no evidence of disease; CMR, complete metabolic response; , male; F, female.

Table 3. Results of histological and immunohistochemical analyses

No.	Grade	LEL	Mitosis	CD20	CD3	CD5	CD10	Bcl-2	Bcl-6	Cyclin D1	LMO2	HGAL	MUM1	IRTA1	CD23	C-myc index	MIB-1 index
Bcl-2$^-$//*IGH-BCL2*$^-$ tFL																	
1	3A	+	Frequent	+	–	–	w+	–	+	–	+	+	–	ND	–	1–2%	80%
2	3A	+	Frequent	+	–	–	w+	–	+	–	+	+	w+	–	w+	10–30%	80%
3	2	+	Frequent	+	–	–	w+	–	+	–	+	+	–	f, w+	–	< 1%	70%
4	3A	+	Frequent	+	–	–	w+	–	w+	–	+	w+	–	w+	–	< 1%	70%
5	3A	+	Frequent	+	–	–	w+	–	+	–	+	+	–	NA	–	< 1%	> 90%
6	2	+	Frequent	+	–	–	w+	–	+	–	+	+	w+	f+	–	1–5%	90%
7	2	+	Frequent	+	–	–	w+	–	+	–	+	+	–	f+	–	5–10%	60%
Bcl-2$^+$//*IGH-BCL2*$^+$ tFL																	
8	3A	+	Rare	+	–	–	+	+	+	–	+	+	–	–	–	1–5%	40%
9	2	+	Rare	+	–	–	+	+	+	–	+	w+	–	–	–	5%	40%
10	1	+	Rare	+	–	–	+	+	+	–	+	+	–	–	–	5%	20–30%
11	3A	+	Rare	+	–	–	+	+	+	–	+	+	–	–	–	1–10%	ND

Bcl-2$^-$//*IGH-BCL2*$^-$ tFL, Bcl-2-negative *IGH-BCL2* translocation-negative follicular lymphoma of the thyroid; Bcl-2$^+$//*IGH-BCL2*$^+$ tFL, Bcl-2-positive *IGH-BCL2* translocation-positive follicular lymphoma of the thyroid; LEL, lympho-epithelial lesion; w, weak; ND, no data; f, focal; NA, not analysable.

© 2021 John Wiley & Sons Ltd. *Histopathology*

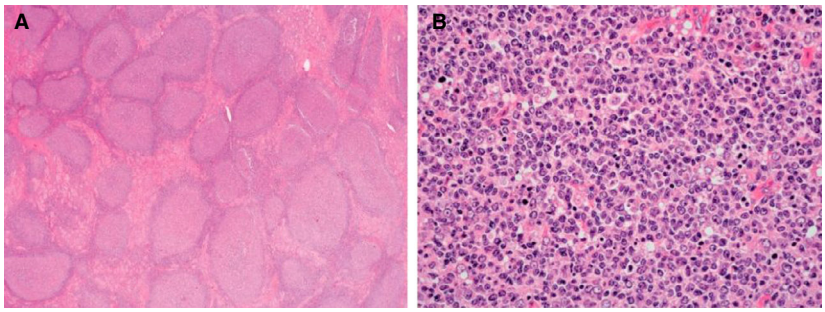

Figure 1. Histology of Bcl-2^{-}/*IGH-BCL2*$^{-}$ follicular lymphoma of the thyroid (tFL) (case 1, haematoxylin and eosin staining). Numerous enlarged lymph follicles were observed in the thyroid tissue (**A**). Centrocyte-like or centroblast-like cells proliferated in expanding germinal centres. Mitosis was frequent (one or more mitotic figures were apparent in one high-power field) (**B**).

Table 4. Results of immunohistochemical analyses for epigenetic modifiers and methylation status of histone

	Epigenetic modifiers				Methylation status of histone	
No.	EZH2	MLL2/KMT2D	CBP/CREBBP	EP300	H3K27me3	H3K4me3
Bcl-2^{-}/*IGH-BCL2*$^{-}$ tFL						
1	w+	+	+	+	-	-
2	+	+	+	+	-	+
3	+	+	+	+	w+	+
4	+	+	+	+	w+	+
5	+	+	+	+	-	+
6	+	+	+	+	-	+
7	+	+	+	+	w+	+
Bcl-2^{+}/*IGH-BCL2*$^{+}$ tFL						
8	w+	+	+	+	w+	+
9	w+	+	-	+	+	+
10	w+	+	+	+	+	+
11	w+	+	-	+	+	+
RLH						
12	+	+	+	+	-	+
13	+	+	+	+	-	+
14	+	+	+	+	-	+

Bcl-2^{-}/*IGH-BCL2*$^{-}$ tFL, Bcl-2-negative *IGH-BCL2* translocation-negative follicular lymphoma of the thyroid; Bcl-2^{+}/*IGH-BCL2*$^{+}$ tFL, Bcl-2-positive *IGH-BCL2* translocation-positive follicular lymphoma of the thyroid; RLH, nodal reactive lymphoid hyperplasia; w, weak.

missense mutation (p. Pro494Thr, case 8) and frameshift insertion (p. Ser1587fs and p. Arg1636fs, case 9) of *ARID1A*, nonsense mutation (p. Gln4322Ter, case 10) and frameshift deletion (p. Glu1957fs, case 9) of *MLL2/KMT2D* and missense mutation (p. Tyr646Phe, case 9) of *EZH2*, nonsense mutation (p. Tyr816Ter, case 8; p. Tyr816Ter, case 9; p. Gln2430Ter, case 10; p. Tyr816Ter, case 10) of *MLL3/KMT2C* were observed in our Bcl-2^{+}/*IGH-BCL2*$^{+}$ tFL cases. Probable pathogenic/pathogenic missense mutation (p. Lys1299Gln, case 4), nonsense mutations (p. Gln1632Ter, case 2; p. Glu1909Ter

© 2021 John Wiley & Sons Ltd, *Histopathology*

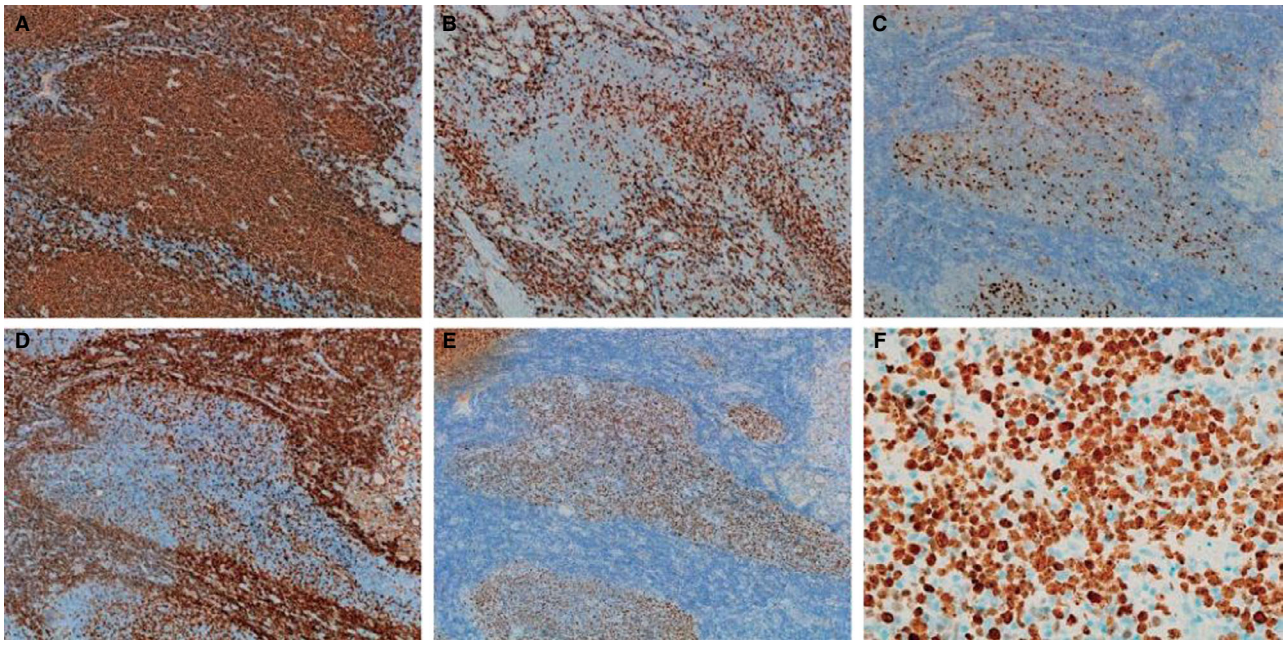

Figure 2. Representative images of immunohistochemical analyses of Bcl-2^{-}/*IGH-BCL2*$^{-}$ follicular lymphoma of the thyroid (tFL). Tumour cells were CD20 (+) (**A**), CD3 (–) (**B**), CD10 (weak+) (**C**), Bcl-2 (–) (Bcl-2-positive T cells were included in germinal centre) (**D**) and Bcl-6 (+) (**E**) (case 7). The MIB-1 labelling index was 80% (case 2) (**F**).

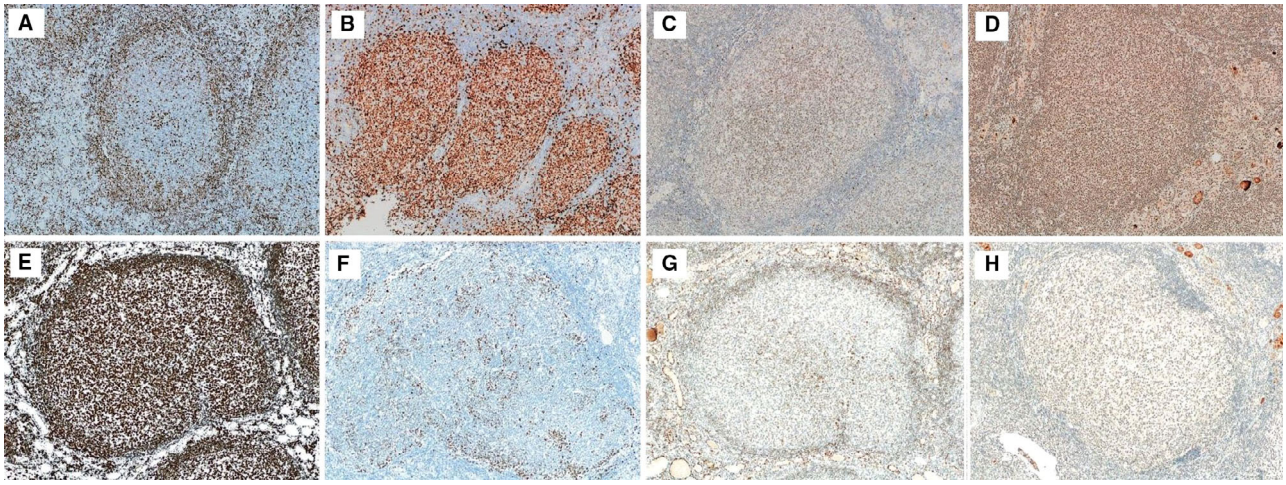

Figure 3. Representative images of immunohistochemical analyses for epigenetic modifiers and methylation status of histones. Bcl-2^{-}/*IGH-BCL2*$^{-}$ follicular lymphoma of the thyroid (tFL) exhibited negative staining for H3K27me3 (case 1) (**A**), positive staining for EZH2 (case 2) (**B**), positive staining for CBP/CREBBP (case 1) (**C**) and positive staining for MLL2/KMT2D (case 1) (**D**). Bcl-2^{+}/*IGH-BCL2*$^{+}$ tFL of the thyroid exhibited positive staining for H3K27me3 (case 9) (**E**), weakly positive staining for EZH2 (case 10) (**F**), negative staining for CBP/CREBBP (case 9) (**G**) and positive staining for MLL2/KMT2D (case 9) (**H**).

case 3), splice site mutation (case 10), frameshift insertion (p. Tyr1255fs, case 3; p. Thr1183fs case 1) and frameshift deletion (p. Ter2003fs, case 2) of *TET2* were observed in Bcl-2^{-}/*IGH-BCL2*$^{-}$ tFLs, but not in Bcl-2^{+}/*IGH-BCL2*$^{+}$ tFLs, except in case 10. Probable pathogenic/pathogenic missense mutation (p. Thr1452Met, Case 1) and frameshift deletion (p. Gln2727fs, case 3; p. Gln2727fs, case 10) of *EP400* were also observed in Bcl-2^{-}/*IGH-BCL2*$^{-}$ tFLs, but not in Bcl-2^{+}/*IGH-BCL2*$^{+}$ tFLs, except in case 10. These mutations have not been previously reported as pathogenic mutations in FLs. Probable

© 2021 John Wiley & Sons Ltd, *Histopathology*

Table 5. Results of the PCR-based gene rearrangement study and FISH analyses

No.	PCR		FISH
	IGH clonal rearrangement	*IGH-BCL2* translocation	*BCL2* rearrangement
Bcl-2$^-$/*IGH-BCL2*$^-$ tFL			
1	+	–	ND
2	+	–	–
3	+	–	–
4	+	–	–
5	+	–	ND
6	+	–	ND
7	–	–	ND
Bcl-2$^+$/*IGH-BCL2*$^+$ tFL			
8	+	+	+
9	+	–	+
10	NA	NA	+
11	NA	NA	+

Bcl-2$^-$/*IGH-BCL2*$^-$ tFL, Bcl-2-negative *IGH-BCL2* translocation-negative follicular lymphoma of the thyroid; Bcl-2$^+$/*IGH-BCL2*$^+$ tFL, Bcl-2-positive *IGH-BCL2* translocation-positive follicular lymphoma of the thyroid; NA, not analysable; ND, no data.

pathogenic/pathogenic missense mutations of *CBP/CREBBP* were detected in one case in each of Bcl-2$^-$/*IGH-BCL2*$^-$ and Bcl-2$^+$/*IGH-BCL2*$^+$ tFLs (p. Ser2382Phe, case 1 and p. Ser2382Phe, case 10, respectively). Mutations in *FGFR3* (p. Val684Ile) and *GATA2* (p. His323Tyr) were recurrently observed in seven specimens of Bcl-2$^-$/*IGH-BCL2*$^-$ and Bcl-2$^+$/*IGH-BCL2*$^+$ tFLs (cases 1–4, 8–11). These mutations were reported to be pathogenic according to OncoKB[16] and COSMIC version 91,[17] but we reserved the conclusion regarding their pathogenicity because the judgements of these databases were based on only one reference.[18]

Discussion

IGH-BCL2$^-$ FLs account for 10–15% of FLs.[4] The prognosis for *IGH-BCL2*$^-$ FL was reported to be better than that for common FL.[4] Bcl-2$^-$/*IGH-BCL2*$^-$ tFL often presents with WHO grade 3 histology and CD10-negative immunohistochemistry, and a similar variant of FL has been described at other extranodal sites, such as the skin or testes.[3] Epigenetic mutations are commonly reported in FL; however, these mutations are infrequent in *IGH-BCL2* translocation-negative FL.[4]

Recent studies have demonstrated that B cell lymphomas originating from germinal centre cells, such as FL, often harbour epigenetic alterations, particularly chromatin remodelling. In our study, Bcl-2$^+$/*IGH-BCL2*$^+$ tFL exhibited low or no immunohistochemical positivity of molecules related to epigenetic modification, probably owing to mutation and overexpression of H3K27me3. Nodal Bcl-2$^+$ FL also exhibited aberrant expression of epigenetic modifiers and abnormal methylation status of histones similar to Bcl-2$^+$/*IGH-BCL2*$^+$ tFL (Supporting information, Table S4), suggesting common oncogenic mechanisms. However, Bcl-2$^-$/*IGH-BCL2*$^-$ tFL did not exhibit H3K27me3 overexpression. In addition, Bcl-2$^-$/*IGH-BCL2*$^-$ tFL retained immunohistochemical positivity for EZH2; therefore, methylation of H3K27 induced by mutated EZH2 is not involved in the oncogenesis of Bcl-2$^-$/*IGH-BCL2*$^-$ tFL. Immunohistochemical positivity for other epigenetic modifiers, MLL2/KMT2D, CBP/CREBBP and EP300 was also retained in Bcl-2$^-$/*IGH-BCL2*$^-$ tFL. These immunohistochemical findings suggest that epigenetic abnormalities common to Bcl-2$^+$/*IGH-BCL2*$^+$ tFL and nodal Bcl-2$^+$ FL may not play a role in the development of Bcl-2$^-$/*IGH-BCL2*$^-$ tFL.

Targeted sequencing analysis demonstrated that Bcl-2$^-$/*IGH-BCL2*$^-$ tFLs do not have pathogenic mutations of epigenetic modifiers, such as *EZH2*, *MLL2/KMT2D*, *MLL3/KMT2C*, *EP300* and *ARID1A*, which have been reported in FLs in the literature,[4] whereas Bcl-2$^+$/*IGH-BCL2*$^+$ tFLs exhibit probably pathogenic/-pathogenic missense mutations or frameshift mutations of these genes. However, Bcl-2$^-$/*IGH-BCL2*$^-$ tFLs are probably pathogenic mutations of other epigenetic modifiers, *TET2* and *EP400*, which have never been observed previously in FLs. These findings suggest that Bcl-2$^-$/*IGH-BCL2*$^-$ tFLs play an oncogenic role in the different genetic and/or epigenetic mechanisms of Bcl-2$^+$/*IGH-BCL2*$^+$ tFLs and other FLs.

TET2 promotes DNA demethylation and modulates the epigenetic status. Somatic mutations in *TET2* have been commonly observed in leukaemias and lymphomas, including angioimmunoblastic T cell lymphomas, mantle cell lymphomas and diffuse large B cell lymphomas.[19] We detected p. Gln1632Ter (nonsense mutation) and p. Lys1299Gln (missense mutation) in cases 2 and 4 as probably pathogenic mutations. These mutations are located within the oxygenase domains of the 2-oxoglutarate and iron (II)-dependent dioxygenase (2OGFeDO) superfamily, which modifies nucleic acids.[20] These variants have been previously reported in polycythaemia vera (p.

© 2021 John Wiley & Sons Ltd, *Histopathology*

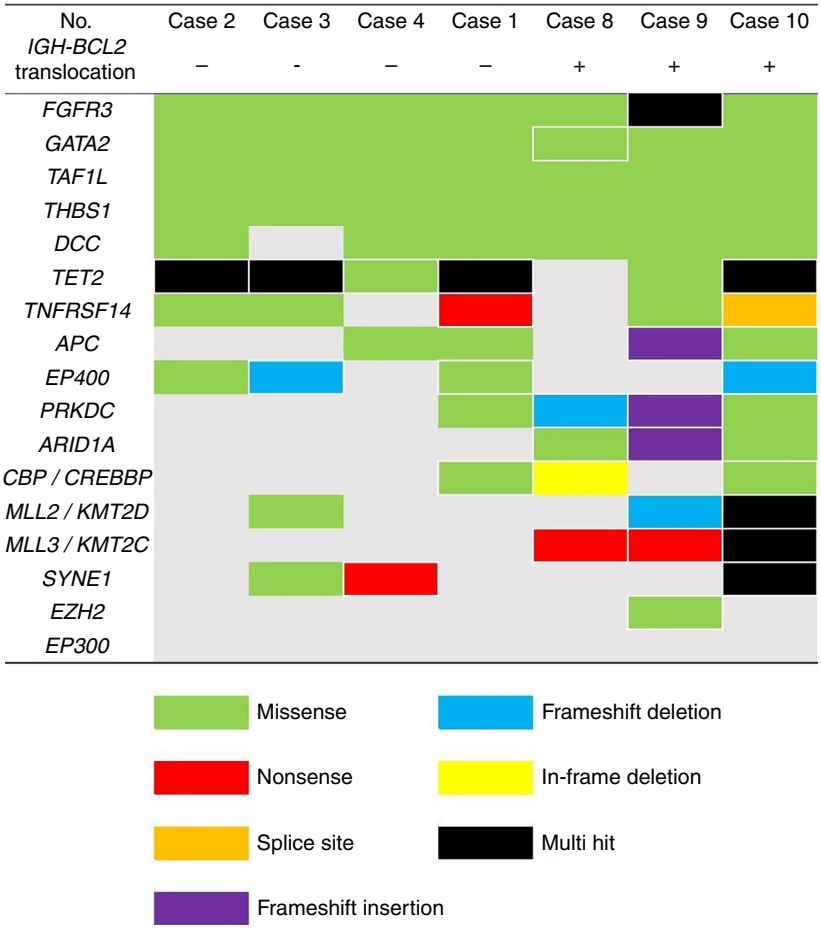

Figure 4. Oncoplot in targeted sequencing. Recurrently mutated genes ranked in the top fifteen and *EZH2* and *EP300* are shown. Mutations which were considered probably pathogenic/pathogenic based on databases (OncoKB, COSMIC version 91 and ClinVar), frameshift mutations, nonsense mutations and splice site mutation are emphasised with a white frame.

Gln1632Ter) and myelodysplastic-myeloproliferative neoplasm (p. Lys1299Gln), and classified as 'pathogenic' in the Catalogue of Somatic Mutations in Cancer (COSMIC) version 91.[17]

EP400 is a chromatin remodelling protein that promotes histone acetylation to control the epigenetic status.[21] Somatic mutations in *EP400* have been observed in bladder cancer and lymphoblastic leukaemia.[22] We detected p. Thr1452Met (missense mutation) in case 1. This mutation has been previously reported in a gastric adenocarcinoma study[23] and classified as 'pathogenic' in COSMIC version 91.[17]

Missense mutations in *FGFR3* (p. Val684Ile) and *GATA2* (p. His323Tyr) are frequently detected in tFLs, regardless of *IGH-BCL2* translocation. The specific pathogenicity of tFL in these genes is unknown, although *GATA2* regulates haematopoietic proliferation and differentiation,[24] and somatic mutations in *GATA2* have been observed in leukaemias.[25]

Different genetic and epigenetic abnormalities in Bcl-2^{-}/*IGH-BCL2*$^{-}$ FLs from Bcl-2^{+}/*IGH-BCL2*$^{+}$ FLs might result from suppression of Bcl-2; alternatively, these abnormalities might be specific spots that were susceptible to mutagenic events in Bcl-2^{-}/*IGH-BCL2*$^{-}$ FLs, but we could not show decisive evidence for these possibilities. Zamo et al. reported that mutations of epigenetic modifiers, such as *CBP*/*CREBBP*, *EZH2* and *EP300*, were found in *IGH-BCL2*$^{-}$ FL,[26] although the localisation of FLs was not specified in their study. They observed enrichment of mutations in the genes associated with N-glycosylation, inflammation and nuclear factor kappa B (NF-κB) signalling, and speculated that increased crosstalk with the microenvironment that may compensate for the lack of N-glycosylation may contribute to oncogenesis of $t_{(14;18)}$-negative FLs. To the best of our knowledge, these mutations have not been previously linked to thyroiditis or other autoimmune diseases. It should

© 2021 John Wiley & Sons Ltd, *Histopathology*

be noted that our study had some limitations. We analysed only exons and, based on this, we could not assess mutations in promoters and introns.

Conclusion

Our study demonstrated differences in aberrations of the expression of epigenetic modifiers and methylation status of histones between Bcl-2^{-}/*IGH-BCL2*$^{-}$ tFL and Bcl-2^{+}/*IGH-BCL2*$^{+}$ tFL. Different genetic and/or epigenetic abnormalities might be involved in the oncogenesis of Bcl-2^{-}/*IGH-BCL2*$^{-}$ tFLs from those associated with Bcl-2^{+}/*IGH-BCL2*$^{+}$ tFLs and other FLs.

Acknowledgements

The authors thank all clinical laboratory technicians in the Department of Clinical Laboratory, OICI; all laboratory members in the Department of Pathology, Osaka University Graduate School of Medicine and all clinical laboratory technicians in the Department of Laboratory Medicine, Kindai University Nara Hospital and Miyoko Higuchi (Kuma Hospital) for their kind technical assistance. The authors also thank Professor Naoki Wada (University of the Ryukyus) and Professor Yoshio Ohta (Kindai University Nara Hospital) for case collection and Editage (http://www.editage.jp) for English language editing. The authors declare no sources of funding.

Conflicts of interest

The authors declare that they have no conflicts of interest.

Data Availability Statement

The data that support the findings of this study are available in the Supporting information for this article.

References

1. Noble VV, Ermann DA, Griffin EK, Silberstein PT. Primary thyroid lymphoma: an analysis of the National Cancer Database. *Cureus* 2019; **11**; e4088.
2. Hirokawa M, Suzuki A, Hashimoto Y *et al*. Prevalence and diagnostic challenges of thyroid lymphoma: a multi-institutional study in non-Western countries. *Endocr. J.* 2020; **67**; 1085–1091.
3. Bacon CM, Diss TC, Ye H *et al*. Follicular lymphoma of the thyroid gland. *Am. J. Surg. Pathol.* 2009; **33**; 22–34.
4. Korfi K, Ali S, Heward JA, Fitzgibbon J. Follicular lymphoma, a B cell malignancy addicted to epigenetic mutations. *Epigenetics* 2017; **12**; 370–377.
5. van Dongen JJM, Langerak AW, Brüggemann M *et al*. Design and standardization of PCR primers and protocols for detection of clonal immunoglobulin and T-cell receptor gene recombinations in suspect lymphoproliferations: report of the BIOMED-2 Concerted Action BMH4-CT98-3936. *Leukemia* 2003; **17**: 2257–2317. https://doi.org/10.1038/sj.leu.2403202.
6. Langerak AW, Groenen PJ, Brüggemann M *et al*. EuroClonality/BIOMED-2 guidelines for interpretation and reporting of Ig/TCR clonality testing in suspected lymphoproliferations. *Leukemia* 2012; **26**; 2159–2171.
7. Karczewski KJ, Francioli LC, Tiao G *et al*. The mutational constraint spectrum quantified from variation in 141,456 humans. *Nature* 2020; **581**; 434–443.
8. Auton A, Brooks LD, Durbin RM *et al*. A global reference for human genetic variation. *Nature* 2015; **526**; 68–74.
9. National Heart, Lung, and Blood Institute (NHLBI) Exome Sequencing Project with 6500 exomes [internet]. Available at: https://evs.gs.washington.edu/EVS/ (accessed 17 July 2020).
10. Tadaka S, Saigusa D, Motoike IN *et al*. jMorp: Japanese multi omics reference panel. *Nucleic Acids Res.* 2018; **46**; D551–D557.
11. Higasa K, Miyake N, Yoshimura J *et al*. Human genetic variation database, a reference database of genetic variations in the Japanese population. *J. Hum. Genet.* 2016; **61**; 547–453.
12. Wang K, Li M, Hakonarson H. ANNOVAR: functional annotation of genetic variants from high-throughput sequencing data. *Nucleic Acids Res.* 2010; **38**; e164.
13. Tohoku Medical Megabank Organization (ToMMo) [internet]. Available at: https://jmorp.megabank.tohoku.ac.jp/201909/downloads/ (accessed 17 July 2020).
14. KJPN Allele Frequency Panel (HGVD) [internet]. Available at: http://www.hgvd.genome.med.kyoto-u.ac.jp/download.html (accessed 17 July 2020).
15. ANNOtate VARiation (ANNOVAR) [internet]. Available at: https://doc-openbio.readthedocs.io/projects/annovar/en/latest/user-guide/download/(accessed 17 July 2020).
16. Precision Oncology Knowledge Base (OncoKB) [internet]. Available at: https://www.oncokb.org/ (accessed 17 July 2020).
17. Catalogue of Somatic Mutations in Cancer (COSMIC v91) [internet]. Available at: https://cancer.sanger.ac.uk/cosmic (accessed 17 July 2020).
18. Chakrabarty S, Varghese VK, Sahu P *et al*. Targeted sequencing-based analyses of candidate gene variants in ulcerative colitis-associated colorectal neoplasia. *Br. J. Cancer* 2017; **117**; 136–143.
19. Solary E, Bernard OA, Tefferi A, Fuks F, Vainchenker W. The ten-eleven translocation-2 (TET2) gene in hematopoiesis and hematopoietic diseases. *Leukemia* 2014; **28**; 485–496.
20. Deepa A, Naveena K, Anindya R. DNA repair activity of Fe(II)/2OG-dependent dioxygenases affected by low iron level in Saccharomyces cerevisiae. *FEMS Yeast Res.* 2018; **18**; 1–8.
21. Fazzio TG, Huff JT, Panning B. An RNAi screen of chromatin proteins identifies Tip60-p400 as a regulator of embryonic stem cell identity. *Cell* 2008; **134**; 162–174.
22. Chen C, Bartenhagen C, Gombert M *et al*. Next-generation-sequencing-based risk stratification and identification of new genes involved in structural and sequence variations in near haploid lymphoblastic leukemia. *Genes Chromosomes Cancer* 2013; **52**; 564–579.

© 2021 John Wiley & Sons Ltd, *Histopathology*

23. ICGC Data Portal [Internet]. International Cancer Genome Consortium. Study ID COSU541: Available from: https://dcc.icgc.org/projects/STAD-US
24. Coma S, Allard-Ratick M, Akino T, van Meeteren LA, Mammoto A, Klagsbrun M. GATA2 and Lmo2 control angiogenesis and lymphangiogenesis via direct transcriptional regulation of neuropilin-2. *Angiogenesis* 2013; **16**; 939–952.
25. Zhang SJ, Ma LY, Huang QH *et al*. Gain-of-function mutation of GATA-2 in acute myeloid transformation of chronic myeloid leukemia. *Proc. Natl Acad. Sci USA* 2008; **105**; 2076–2081.
26. Zamò A, Pischimarov J, Schlesner M *et al*. Differences between BCL2-break positive and negative follicular lymphoma unraveled by whole-exome sequencing. *Leukemia* 2018; **32**; 685–693.

Supporting Information

Additional Supporting Information may be found in the online version of this article:

Table S1. The list of 409 targeted genes.

Table S2. The list of all the extracted mutations.

Table S3. Clinical findings of nodal Bcl-2-positive follicular lymphoma.

Table S4. Results of immunohistochemical analyses for epigenetic modifiers and methylation status of histone in nodal Bcl-2-positive follicular lymphoma.

© 2021 John Wiley & Sons Ltd, *Histopathology*